NIR spectral–kinetic analysis for thermally degraded Sugi (*Cryptomeria japonica*) wood

Tetsuya Inagaki[1] · Miyuki Matsuo[1] · Satoru Tsuchikawa[1]

Abstract Kinetic analysis was conducted on principal component scores calculated from second-derivative near-infrared (NIR) spectra of thermally treated Sugi (*Cryptomeria japonica*) wood samples. NIR reflectance spectra were measured for wood samples thermally treated at 90, 120, 150 and 180 °C in an air-circulating oven for periods ranging from 5 min to approximately 1.4 years. The Arrhenius approach, which involves the time–temperature superposition method, is used to understand the change in the principal component score. The master curve corresponded well with the change in principal component scores at each temperature and yielded a determination coefficient between the measured and estimated data of 0.99 for second principal component score. This report shows that kinetic analysis is useful to understand changes in the principal component score calculated from NIR spectra of wood subjected to thermal treatment.

1 Introduction

The thermal modification of wood has long been carried out to change its properties. There are some advantages such as an increasing of dimensional stability, resistance to fungal decay and coloration. There are many types of thermal modification (wood species, temperature, atmosphere and duration), and their effects on chemical component, strength, moisture content and dimensional stability are reported as summarized by Esteves et al. [1].

The chemical behavior is an important factor affecting other wood properties. It is generally known that 1) hemicellulose and the amorphous region in cellulose are the first chemical compounds to be thermally affected, even at low temperature, 2) crystalline cellulose is less affected, and 3) the lignin content in wood relatively increases with thermal treatment [1]. However, it is difficult to make prevailing prediction of the treatment result in detail due to the various chemical natures of wood species. For the effective thermal treatment of wood for industrial purpose, nondestructive method of wood chemical component is required.

Near-infrared (NIR) spectroscopy has been reported to have a high application potential as a nondestructive tool in the wood products industry for the rapid determination of chemical, mechanical and physical properties of wood [2, 3]. Evaluation of thermally treated wood has been attempted using NIR spectroscopy. Bächle et al. [4] fully investigated the NIR second-derivative change in beech and spruce with thermal treatment with 180–220 °C. They reported the good prediction for oven-dry and basic density, MOE and MOR from NIR spectroscopy with partial least square (PLS) regression analysis. In another paper, a good classification of thermally modified wood samples according to the treatment intensity with soft independent modeling of class analogies (SIMCA) was constructed by Bächle et al. [5]. Windensen et al. [6] investigated the relation between chemical change determined by mean of several methods including NIR spectroscopy and mechanical properties of thermally treated wood. Esteves et al. [2] reported that many wood properties in thermally treated wood can be predicted by NIR spectroscopy with PLS regression analysis.

The critical problem for the application of NIR spectroscopy for wood science is the complexity of NIR spectra

✉ Tetsuya Inagaki
  inatetsu@agr.nagoya-u.ac.jp

[1] Graduate School of Bioagricultural Sciences, Nagoya University, Furo-cho, Chikusa-ku, Nagoya 464-8601, Japan

of wood as a complex polymer. Absorption in the NIR region results from harmonics or overtones of the fundamental absorption of molecular vibration. Broad absorption and the influence of the physical condition of a sample can make spectra difficult to analyze. Multivariate statistical methods based on the projection of spectral information to latent structures, such as principal component analysis (PCA) and PLS regression, are promising for the quantitative and qualitative analysis of such complex data. To prepare a robust calibration curve, training samples set should have a sufficient range of the properties under evaluation and represent all the important sources of variability that would be included in the samples to be predicted. When wood is measured in the reflectance mode, important factors include the wood species, moisture content, density, and surface roughness. A large number of samples are necessary to cover the variability of such properties. Therefore, we propose a new method that combines the unsupervised analysis of spectral and kinetic analysis. The NIR spectral change with thermal treatment of wood can be predicted by using the method.

Kinetic analysis is a method used to explain the temperature dependence of the reaction rate in chemical reactions. In wood science, the application of kinetic analysis has been demonstrated to enable the prediction of pyrolysis or deterioration of lignocellulose materials [7–11]. An Arrhenius approach has been used for polymers that involve the time–temperature superposition (TTSP) method to derive the shift factors and understand the Arrhenius behavior [12].

In this study, PCA was employed with the aid of kinetic analysis to understand the change in NIR spectra for wood that was heat treated under dry conditions. The loading vectors were calculated, which indicate the direction of NIR spectral change due to the thermal oxidation of wood. Arrhenius plots were employed to calculate the activation energy.

2 Materials and methods

2.1 Samples

Thermally treated wood samples, as reported by Matuso et al. [13], were adopted. Samples were cut from a 180-year-old Sugi (*Cryptomeria japonica* D. Don) tree into small pieces [60 mm (longitudinal direction) × 10 mm (radial direction) × 2 mm (tangential direction)]. The wood specimens were dried in an air-circulating oven and a vacuum oven at 60 °C for 24 h. Then, the specimens were thermally treated at 90, 120, 150 and 180 °C in an air-circulating oven for periods ranging from 10 min to approximately 1.4 years, as summarized in Table 1. A sample block of homogenous grain for each species was carefully selected from the area near the outermost part of the heartwood. Each species

Table 1 Treatment temperatures and time

90 °C (h)	120 °C (h)	150 °C	180 °C
85.3	10.7	40 min	5 min
171	21.3	1.33 h	10 min
256	32	2.67 h	20 min
384	48	4 h	30 min
524	64	6 h	1 h
1024	124	8 h	1.5 h
3072	384	16 h	2 h
6144	768	48 h	6 h
9266	1536	96 h	7 h
12,288	5440	192 h	12 h
	7680	384 h	24 h
		960 h	48 h
			84 h
			120 h

covers 5–10 annual growth rings. Four samples were obtained for each thermal treatment condition.

2.2 NIR measurement

NIR reflectance spectra were measured from the radial face of the air-dried wood samples using a Fourier transform (FT)-NIR spectrophotometer (Bruker MATRIX-F; TE-InGaAs detector with a fiber optic probe with a measurement area of 7 mm^2) under laboratory conditions. This measurement area contains 1 or 2 years of tree rings, where averaged spectral information of earlywood and latewood was acquired. A white plate (barium sulfate) served as the background. To improve the signal-to-noise ratio, 64 scans were co-added at a spectral resolution of 8 cm^{-1} over the wavenumber range 7500–4000 cm^{-1}. A zero-filling of two (corresponding to a spectral interval of 4 cm^{-1}) was applied. Absorbance for the analysis was calculated using the following equation:

$$A = -\log\left(\frac{I}{I_0}\right), \tag{1}$$

where A is the absorbance, I is the reflected light intensity from the sample and I_0 is the reflected light intensity from the white plate background (reference). Three NIR spectral measurements were made and averaged for each sample.

2.3 Data processing: multivariate data analysis and kinetic analysis

MATLAB (MathWorks, Inc., MA, USA) was used for spectral data preprocessing, calculation of the PCA score and kinetic analysis. NIR spectra were processed

(smoothed and derived) using a 21-point smoothing filter and a second-order polynomial to obtain second derivatives (Savitzky-Golay, second derivative). PCA of second-derivative NIR spectra of wood was conducted without mean-centering of the data.

3 Results and discussion

3.1 NIR second-derivative spectra

Figure 1a, b shows the second-derivative NIR spectra for the control wood (black solid line), wood treated at 150 °C for 48 h (blue solid line) and wood treated at 180 °C for 120 h (red solid line). The absorption bands in the NIR region are conclusively associated with three polymers in wood: cellulose, hemicellulose and lignin, and water and extractives. The absorption band characteristics of the wood samples are labeled, and their assignments are summarized in Table 2. The assignments in Table 2 refer to Schwanninger et al. [14]. They summarized the knowledge about the assignment of NIR absorption peaks for wood by reviewing the 70 years of NIR band assignment literature for wood and wood components.

For second-derivative spectra, lower absolute amplitudes of second-derivative values correspond to lower chemical concentrations. A clear decrease and peak shift toward higher wavelength are evident for the absorption band at 7006 cm^{-1} (peak 1). The difference of second-derivative value around 7000 cm^{-1} with thermal treatment was also reported by Todorović et al. [15] (beech treated at 170, 190 and 210 °C for 4 h under water vapor atmosphere), Windeisen et al. [6] (beech treated at 180, 200 and 220 °C for 4–6 h under oxygen exclusion) and Bächle et al. [4] (beech and spruce treated at 180, 200 and 220 °C for 4 h under oxygen exclusion). Inagaki et al. [16] reported the decrease in second-derivative value at 7000 cm^{-1} also for oven-dried hinoki wood with hydrothermal treatment under water vapor atmosphere. On the other hand, decrease in equilibrium moisture content with thermal treatment is well known as reviewed by Esteves et al. [1]. These knowledge imply that the decrease in second-derivative value at 7000 cm^{-1} might be attributed to both the cleavage of OH groups as Mitsui et al. reported [17] and the decrease in equilibrium moisture content of wood.

It is reported that the second-derivative values within the wavenumber region 6020–5770 cm^{-1} correlate well with the lignin contents of milled spruce wood by Schwanninger et al. [14]. The absorption bands at 5987 cm^{-1} (peak 4) and 5886 cm^{-1} (peak 5), which are attributable to C–H vibrations for aromatic rings/O–H groups in hemicellulose and methyl/methylene groups in

lignin, hemicellulose and cellulose, decreased and the peaks shifted to higher wavenumber with thermal treatment. No drastic change at 5880 cm^{-1}, assigned to first overtone of O–H vibration in lignin, hemicellulose and cellulose with thermal treatment, was observed. However, Windeisen et al. [6] reported the increase in band around 5950 cm^{-1} and decrease in band around 5800 cm^{-1} for thermally treated beech wood. They attribute the increase in band around 5950 cm^{-1} to the relative increase and structural variation of lignin and decrease in band around 5800 cm^{-1} to degradation of polyoses and/or deacetylation of xylan. Furthermore, Bächle et al. [4] also reported feature differences at 5981 cm^{-1} which indicate the modifications in lignin with thermal treatment for spruce. They reported that the NIR spectra of beech wood showed similar features to the spectra of spruce although the difference between before and after thermal treatment is more obvious for beech compared to spruce. The difference for the spectral behavior at the range of 6020–5700 cm^{-1} with thermal treatment observed in this study might be because of lower thermal treatment temperature. The study by the Windeisen et al. and Bächle et al. implies the lignin modifications at 180–220 °C although lignin has been supposed to be comparatively stable at higher temperature. However, lignin might not be modified at the lower temperature (90–180 °C) used in this study as confirmed by thermogravimetric data [9], although the hemicellulose was thought to be affected even at low temperature that leads to the decrease in band at 5950 and 5880 cm^{-1}. New extractives resulting from the degradation of hemicellulose and amorphous cellulose [1] also might affect to the absorption band in this range.

The absorption bands at 5226 cm^{-1} (peak 8) assigned to OH vibration in water shifted toward higher wavelength. The peak position of water reflects the state of water contained in the wood sample, where a higher wavenumber peak position corresponds to weaker hydrogen bonding between water molecules or the OH groups in wood. The equilibrium moisture content of aged or thermally treated wood is known to be lower than that of modern or non-heated wood when exposed to the same climate. The water adsorption/desorption mechanism in modern and archaeological wood was investigated according to the decomposition of the OH absorption band at 5226 cm^{-1} into three components (free water molecules, those with one OH group engaged in hydrogen bonding and those with two OH groups engaged in hydrogen bonding) [18]. The peak shift to higher wavenumber observed in this study corresponds well with this conclusion, where adsorbed water molecules in a modern wood sample are more strongly hydrogen bonded than those in archaeological wood samples.

Fig. 1 **a**, **b** NIR second-derivative spectra for control wood (*black solid line*), wood treated at 150 °C for 48 h (*blue solid line*) and wood treated at 180 °C for 120 h (*red solid line*). The numbers correspond to the assignments given in Table 2. We used different scales in **a** 7200–5500 cm^{-1} and **b** 5500–4000 cm^{-1} in order to clearly show the change in second-derivative spectra with thermal treatment. Loading coefficients of **c**, **d** PC1, **e**, **f** PC2, **g**, **h** PC3 and **i**, **j** PC4 calculated from the PCA
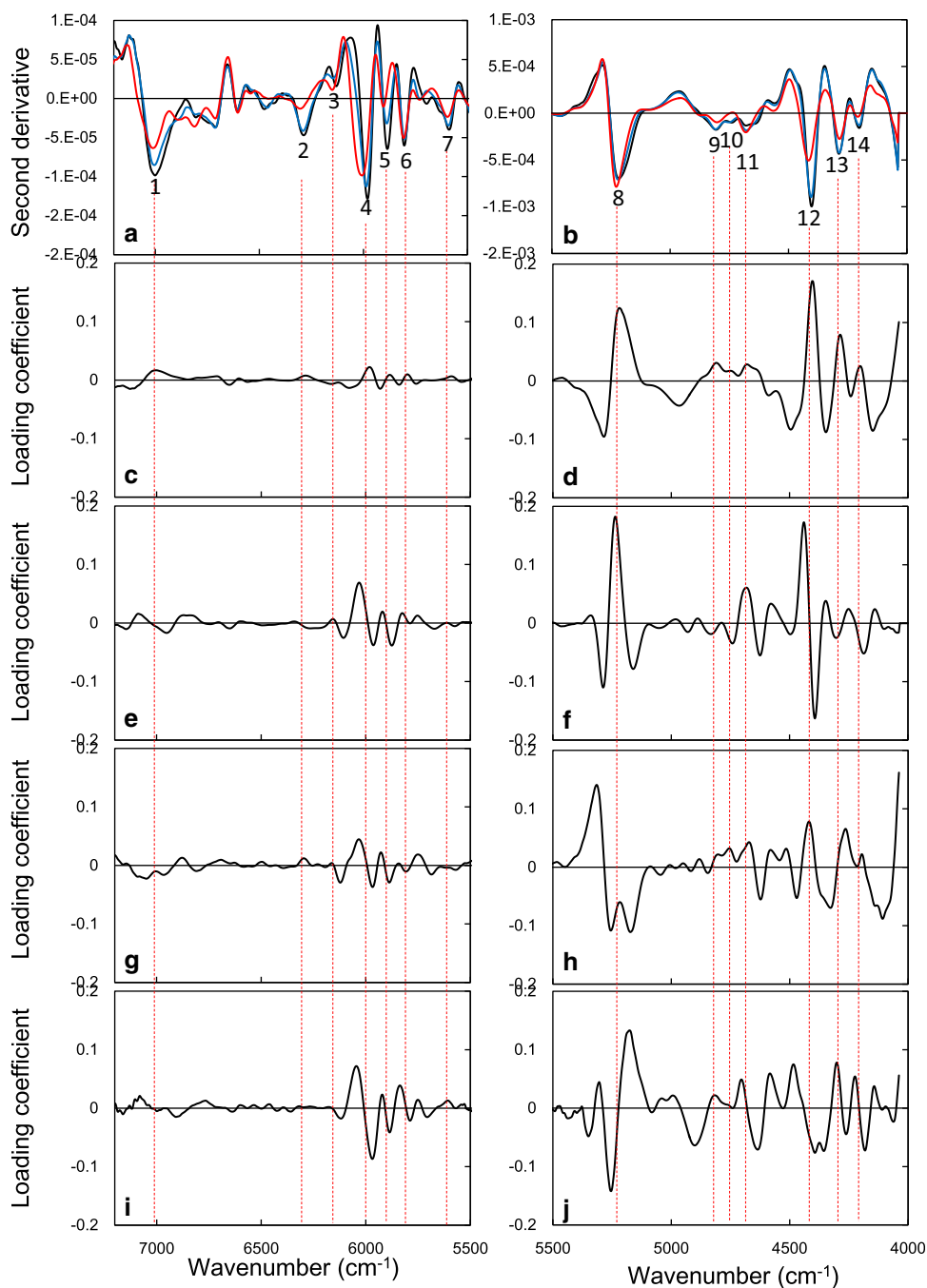
3.2 Kinetic analysis for PCA score

PCA is a linear method that allows the projection of multi-dimensional data onto a few orthogonal features, i.e., principal components (PCs). The second-derivative spectra of a wood sample within 7500–4000 cm^{-1} were subjected to PCA. Calculated loading of PC1, PC2, PC3 and PC4, which represents 98.9, 0.9, 0.059 and 0.038 %, respectively, of the spectral data variance, is shown in Fig. 1c–j. PC2, PC3 and PC4 represent only a small percent of the

spectral data variance because PCA was conducted without mean-centering of the data. We tried the calculation of PCA score also with mean-centering of spectral data; however, the variation of PCA scores within same thermal treatment condition (i.e., variance within four samples) was much bigger compared with PCA scores conducted without mean-centering.

Leverage correction validation was applied to determine the optimum number of PCs. The determined optimum number was 1. However, the score change with thermal

Table 2 Band assignments, determination coefficients (r^2) and activation energies [E_a (kJ mol^{-1})] from peak positions and intensities of second-derivative spectra

	Wavenumber (cm^{-1})	Assignment	Component	Wavenumber from reference (cm^{-1})	Peak position R^2	Peak position E_a	Second-derivative value R^2	Second-derivative value E_a
1	7020–6998	1st OT O–H str. + H$_2$O	Amorphous regions in cell., water	7003–6993	–	–	0.829	110.73
2	6290	1st OT O–H str.	Crystalline cell. II	6307–6267	–	–	0.868	125.30
			Strong O(2)–H(2)···O(6) of cell	6300–6295				
			Crystalline region in cell	6281				
3	6150–6130	1st OT O–H str.	Cell	6126	0.845	90.83	–	–
4	6012–5980	1st OT O–H str.	Hemi.	6003	0.948	99.42	–	–
		1st OT C$_{arm}$–H str.	Lig.	5980@@5974@@5963@@5978				
5	5902–5885	1st OT O–H str.	–	5900	0.897	109.91	0.856	104.15
		1st OT C–H str.	Lig.	5890				
		1st OT C–H str.	Cell	5872				
		1st OT O–H str.	Hemi.	5865				
6	5807–5803	1st OT O–H str.	Lig./Hemi./Cell	5814, 5816	–	–	–	–
			Hemi.	5800				
			Lig.	5795				
7	5590	1st OT C–H str.	Cell	5593, 5587	–	–	–	–
			Lig.	5583				
			Cell	5577				
8	5228–5215	2nd OT C=O str.	Hemi.	5245, 5236	0.857	140.25	–	–
		O–H asym. str. + O–H def. of water	Water	5220–5150				
9	4809–4800	O–H str. + C–H def.	Cell	4808	–	–	–	–
10	4744	O–H str. + O–H and C–H def.	Cell./Hemi.	4795	–	–	0.886	127.59
		O–H and C–H def. + O–H str.	Cell	4780–4760				
		O–H and C–H def. + O–H str.	Cell	4762				
		O–H def. + O–H str.	Cell	4739				
11	4684–4680	Car–H str. + C=C str.	Lig./extr.	4686	–	–	0.901	116.97
		C–H str. + C=O str.	Hemi.	4686				
12	4414–4402	O–H str. + C–O str.	Lig.	4411	–	–	0.943	103.73
		O–H str. + C–O str.	Cell	4405				
		C–H$_2$ str. + C–H$_2$ def.	Cell/Hemi.	4404				
		C–H str. + C–H def.	Hemi.	4401				
		O–H str. + C–C str. and/or C–H str. + C–H def.	Cell	4392				

Table 2 continued

Wavenumber (cm^{-1})	Assignment	Component	Wavenumber from reference (cm^{-1})	Peak position R^2	Peak position E_a	Second-derivative value R^2	Second-derivative value E_a
13	4287	C–H str. + C–H def.	Hemi	4296–4288	–	–	0.835	114.73
		C–H str. + C–H def.	Cell/Hemi.	4283@@4281				
		C–H str. + C–H$_2$ def.	Lig.	4280				
		C–H str. + C–H$_2$ def.	Cell	4277				
14	4208–4200	2nd OT O–H def.	Holo.?	4202	–	–	0.885	110.94
		Not assigned	Lig.	4195				

OT overtone, *sym.* symmetric, *asym.* asymmetric, *str.* stretching vibration, *bend* bending vibration, *def.* deformation vibration, *+.* combination band; *Lig.* lignin, *Holo.* holocellulose, *Hemi.* hemicellulose, *Cell.* cellulose, *Extr.* extractives

treatment was explained by kinetic analysis for PC1, PC2, PC3 and PC4 as shown in Figs. 2, 3, 4 and 5. Changes in the (a) score and (b) superimposed score calculated from NIR second-derivative spectra (7500–4000 cm^{-1}) as a function of treatment time and (c) Arrhenius plot of shift factors from empirical superposition of the change in Ln(a_T) are shown in these figures.

Figure 3a shows the change in the PC2 score as a function of the logarithmic thermal treatment time (four samples from each thermal treatment condition, 188 samples in total). The higher temperature accelerates the change in the PC2 scores. When the relation between the thermal treatment time and spectral response is nonlinear as in this case, the PLS regression method, which is the most widely used for spectroscopic analysis, is not suitable for the prediction of NIR spectral change with thermal treatment time. Although many effective nonlinear methods are available, we suggest the use of an Arrhenius approach that involves the TTSP method to interpret the change in the PCA score. The Arrhenius equation has commonly been used to treat a single chemical reaction. However, the degradation process of wood involves multiple reactions; therefore, the calculated activation energy can be regarded as an averaged weight by the rate of each reaction, as reported by Zou et al. [19]. The PCs calculated from NIR spectra represent such multiple reactions; therefore, it was assumed that the behavior of the PC score by thermal treatment can be analyzed using an Arrhenius approach. The temperature dependence of the degradation rate constant is described by the Arrhenius equation:

$$k = A \exp\left(-\frac{E_a}{RT}\right), \tag{2}$$

where A is a frequency factor, E_a is the activation energy (kJ mol^{-1}), R is the gas constant (kJ mol^{-1} K^{-1}) and T is the absolute temperature (K). Thus, the activation energy can be calculated by determination of the degradation rate.

TTSP is the most reliable method to successfully probe for Arrhenius behavior. The time and temperature are equivalent according to the principles of the TTSP method. The parameters measured as a function of thermal treatment time at different temperatures can be superimposed by an appropriate change in scale (referred to as the time–temperature shift factor, a_T) on the time axis. The shift factor a_T is defined as

$$a_T = \frac{t_{ref}}{t_T}, \tag{3}$$

where t_{ref} is the thermal treatment time at a reference temperature T_{ref}, and t_T is the time that gives the same response at temperature T. Combining Eqs. (2) and (3) gives
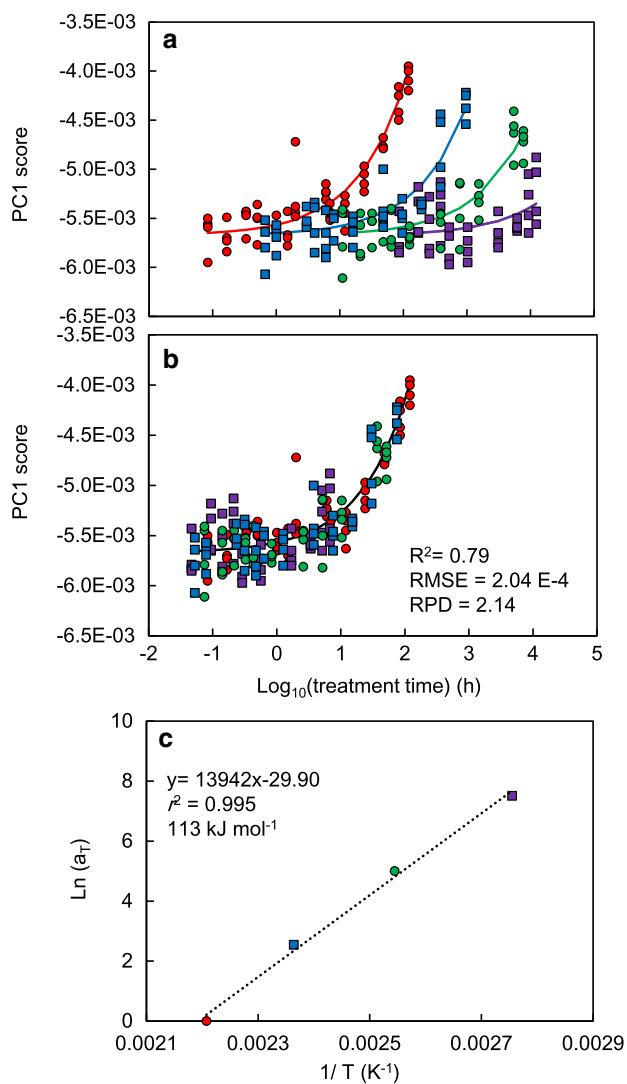
Fig. 2 Changes in the **a** PC1 score and **b** superimposed PC1 score calculated from NIR second-derivative spectra (7500–4000 cm^{-1}) as a function of treatment time. *Purple square*, *green circle*, *blue square* and *red circle* show the score of wood samples treated at 90, 120, 150 and 180 °C, respectively. R^2, *RMSE* and *RPD* show the determination coefficient between the measured and simulated values, root-mean-square error and ratios of performance to deviation. **c** Arrhenius plot of shift factors from empirical superposition of the change in Ln(a_T)
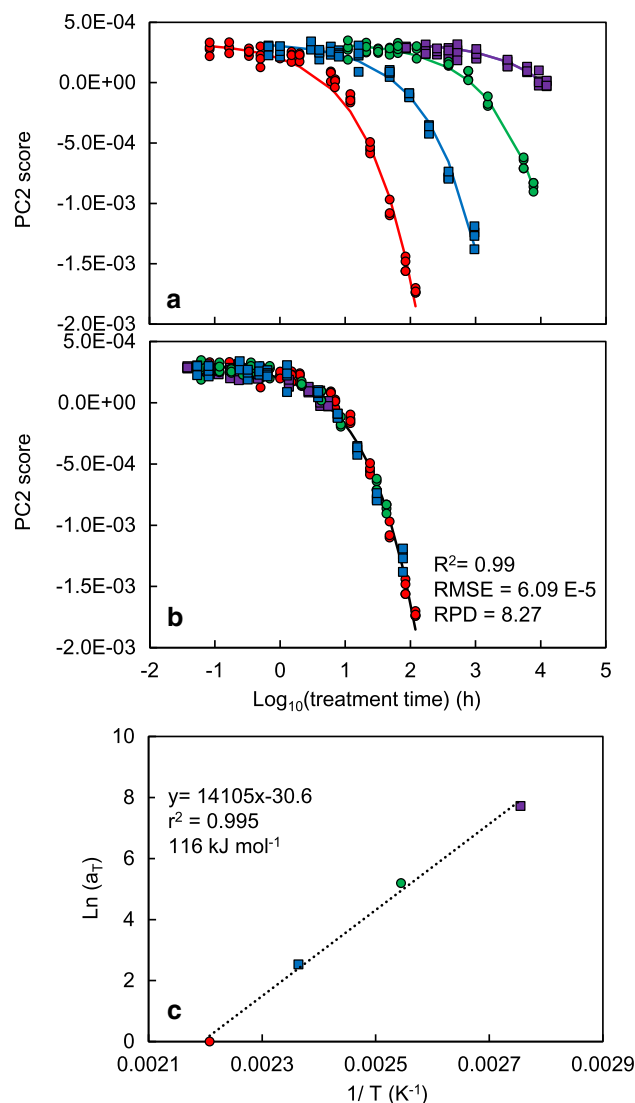
Fig. 3 Changes in the **a** PC2 score and **b** superimposed PC2 score calculated from NIR second-derivative spectra (7500–4000 cm^{-1}) as a function of treatment time. *Purple square*, *green circle*, *blue square* and *red circle* show the score of wood samples treated at 90, 120, 150 and 180 °C, respectively. R^2, *RMSE* and *RPD* show the determination coefficient between the measured and simulated values, root-mean-square error and ratios of performance to deviation. **c** Arrhenius plot of shift factors from empirical superposition of the change in Ln(a_T)

$$a_T = \exp\left[\frac{E_a}{R}\left(\frac{1}{T_{ref}} - \frac{1}{T}\right)\right]. \quad (4)$$

Equation (4) shows that the logarithm of the empirically determined shift factor a_T has a linear relation with the reciprocal absolute temperature (T), which enables E_a to be calculated and the shift factor to be predicted for a desired temperature. The data obtained for 180 °C were first selected as the reference data to determine the master curve over the temperature range. The PCA score for wood treated at 180 °C is selected as the master curve due to the large change with treatment time. The PCA score was

estimated using Eq. (5) with a nonlinear curve-fitting method, i.e., the Nelder–Mead method. A logistic function that adds the one constant (δ) was used as an evaluation function as follows:

$$f(x) = \delta + \frac{\alpha}{1 + \beta \exp(-\gamma x)}, \quad (5)$$

where $f(x)$ is the PCA score, x is log(t_T/a_T), and α, β, γ and δ are constants. After the master equation (α, β, γ and δ) was determined at the experimental temperature of 180 °C ($a_{180 °C} = 1$), the shift factor was determined, which is

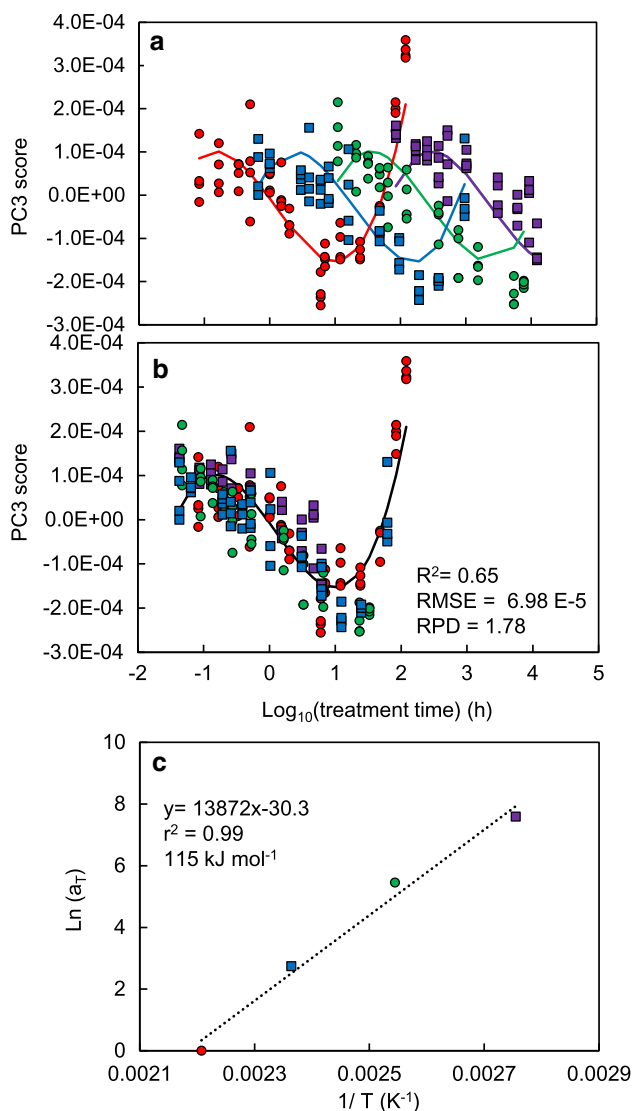**Fig. 4** Changes in the **a** PC3 score and **b** superimposed PC3 score calculated from NIR second-derivative spectra (7500–4000 cm^{-1}) as a function of treatment time. *Purple square*, *green circle*, *blue square* and *red circle* show the score of wood samples treated at 90, 120, 150 and 180 °C, respectively. R^2, *RMSE* and *RPD* show the determination coefficient between the measured and simulated values, root-mean-square error and ratios of performance to deviation. **c** Arrhenius plot of shift factors from empirical superposition of the change in Ln(a_T)

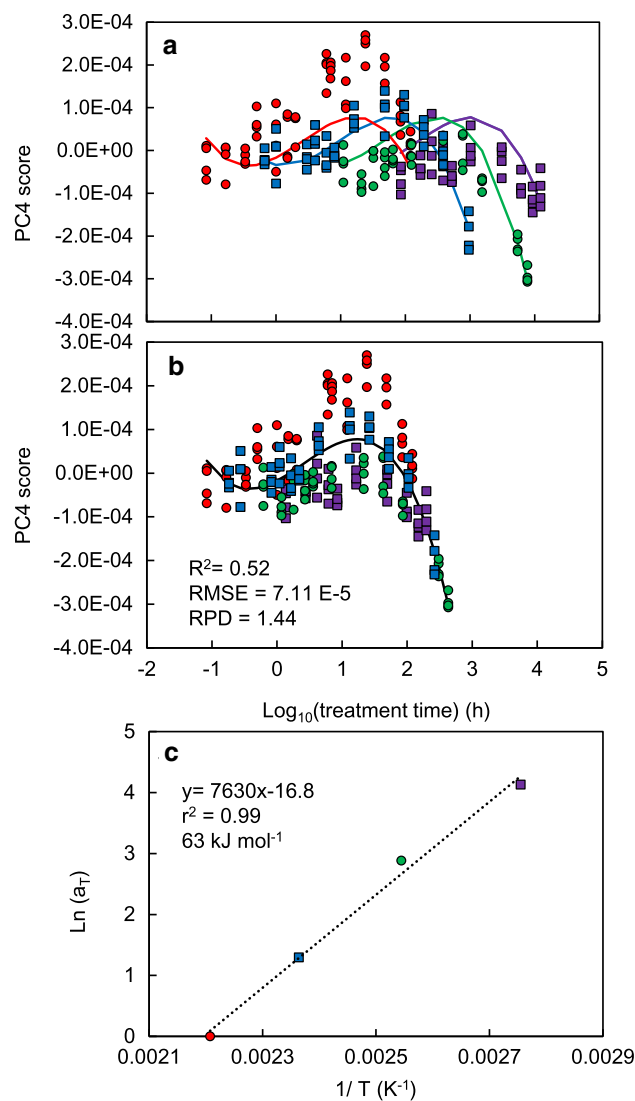**Fig. 5** Changes in the **a** PC4 score and **b** superimposed PC4 score calculated from NIR second-derivative spectra (7500–4000 cm^{-1}) as a function of treatment time. *Purple square*, *green circle*, *blue square* and *red circle* show the score of wood samples treated at 90, 120, 150 and 180 °C, respectively. R^2, *RMSE* and *RPD* show the determination coefficient between the measured and simulated values, root-mean-square error and ratios of performance to deviation. **c** Arrhenius plot of shift factors from empirical superposition of the change in Ln(a_T)

chosen empirically to produce the best overall superposition with the 180 °C data for each temperature (90, 120 and 150 °C).

Figure 3b shows the superimposed PC2 score data with the regression curve. The master curve can be applied to data of each temperature by application of the shift procedure. The determination coefficient (R^2) between the measured and simulated value by the superimposed curve was 0.99. The root-mean-square error (RMSE) from the superimposed curve was 6.09×10^{-5}. R^2 and RMSE are defined as

$$R^2 = 1 - \frac{\sum\left(y - y_{\text{pred}}\right)^2}{\sum\left(y - \bar{y}\right)^2}, \tag{6}$$

$$\text{RMSE} = \sqrt{\frac{\sum\left(y - y_{\text{pred}}\right)^2}{n - 1}}, \tag{7}$$

where y is PCA score value, $\bar{y}$ is average of y, y_{pred} is the y value predicted using the TTSP method and n is the number of y. The high value of the determination coefficient implies the change in PC2 is caused by the same process independent of the thermal treatment temperature.

The loading spectra, which may be regarded as the vector of wood degradation by thermal treatment, for PC2 (see Fig. 1e–f) reveals that the highest loading is in the water absorption (peak 8) and combination band (peak 11). The loading coefficient values at the wavelength of peak 1, 4, 5, 12 and 14, which showed the peak shift with thermal treatment, are close to zero. Figure 3c shows the relation between $\ln(a_T)$ and $1/T$. The apparent activation energy derived from the slope of regression line was 116 kJ mol^{-1}, which is similar to those obtained for some wood properties such as weight reduction, modulus of elasticity and modulus of rupture (110–130 kJ mol^{-1}).

Arrhenius approach was also adopted for PC1, PC3 and PC4 using the TTSP method as shown in Figs. 2, 4 and 5. Results are summarized in Table 3. R^2 was the highest when PC2 was used. For PC3 and PC4, a third-order polynomial expression was selected after Eq. (5) failed to provide a good fit. PC1 score and PC3 score were explained by superimposed curves indicating that the degradation process was independent to thermal treatment temperature, although the R^2 is not high because of the variance of score within same thermal treatment condition (i.e., variance within four samples). PC4 score was not successfully explained by superimposed curve, where the scores of samples treated at 180 °C are underestimated and scores of samples treated at 90 and 120 °C are overestimated. This result implies the different chemical processes depend on the temperature. The loading spectra for PC3 and PC4 showed complex feature, while that of PC1 was almost the same shape as second-derivative spectra of wood.

As we explained, training samples set should have a sufficient range of the properties under evaluation and represent all the important sources of variability that would be included in the samples to be predicted to prepare a robust calibration curve by PLS or PCA regression analysis. For example, we should not use the PLS or PCA calibration curve constructed using the samples treated at 120 °C for the prediction of property in wood samples treated at 150 °C. In this study, however, we showed that PC2 is caused by the same process independent of the thermal treatment temperature, implying that we can estimate the 'thermal treatment degree' of wood samples treated at any temperature between 90 and 180 °C (i.e., 135 °C) using constant α, β, γ, δ and shift factor a_T in

Eq. (5) determined in this study. Of course, we need further research using more sample treated at various kinds of temperatures to confirm that.

3.3 Kinetic analysis for second-derivative spectra evaluation of spectral noise

The peak positions (cm^{-1}) and their second-derivative values were used for the kinetic analysis fitted by Eq. (5). For the second-derivative spectra, higher wavenumber peak positions correspond to higher band energies, while lower amplitudes of the second-derivative value correspond to lower chemical concentrations in wood. The results are shown in Table 2, where only the results that produced a determination coefficient higher than 0.8 are presented. All of the determination coefficient values were smaller than the result of the PC2 score. However, the activation energy calculated for second-derivative bands gave beneficial information. As the activation energy is defined as the energy required to start the chemical reaction, kinetic analysis for second-derivative spectra allows the simultaneous evaluation of resistance of each functional group to thermal treatment. For example, it was reasonable that the activation energy for second-derivative value at the bands of peak 1 (amorphous region in cellulose or water: 110.73 kJ mol^{-1}) are smaller compared with peak 2 (crystalline region in cellulose: 125.30 kJ mol^{-1}). The application of Arrhenius approach for the second-derivative spectra of wood allows the simultaneous prediction of activation energy of many functional groups in wood.

The determination of the noise source in terms of deviation of PC2 score from superimposed curve leads to the understanding of the prediction error. Therefore, the spectrophotometer noise was measured; NIR reflection light intensity from the white plate was measured 11 times. We calculated absorbance regarding the light intensity recorded at first as the reference, and others as light intensity of sample as equation:

$$A_i = -\log\left(\frac{I_i}{I_1}\right) \tag{8}$$

where, the A_i is absorbance at i_{th} measurement ($i = 2$–11), I_1 is reflection light intensity of white plate measured at first and I_i is reflection light intensity of white plate at i th

Table 3 Determination coefficients for PCs determined by kinetic analysis

PC	Approximate function	Variance of second spectral variance (%)	R^2
PC1	$f(x) = \delta + \frac{\alpha}{1 + \beta \exp(-\gamma x)}$	98.9	0.79
PC2	$f(x) = \delta + \frac{\alpha}{1 + \beta \exp(-\gamma x)}$	0.90	0.99
PC3	$f(x) = \alpha x^3 + \beta x^2 + \gamma x + \delta$	0.059	0.65
PC4	$f(x) = \alpha x^3 + \beta x^2 + \gamma x + \delta$	0.038	0.52

measurement ($i = 2$–11). The calculated absorbance (defined as noise spectra) was almost zero, but included a slight deviation from zero due to detector noise, photon noise and modulation noise. The second-derivative was applied to the noise spectra, and the score was calculated using PC2 loading. The maximum score value of ten noise spectra was 5.80×10^{-7}, and the standard deviation was 2.73×10^{-7}, which is relatively small compared to the calculated RMSE (6.09×10^{-5}). This result indicates that the deviation from the superimposed curve shown in Fig. 3 is mainly attributable to the spatial distribution of chemical components in the wood samples, i.e., earlywood and latewood, or the variability between specimens. The prediction accuracy might be improved if the samples used were homogenized (physical structure).

The use of thermally treated wood or paper to simulate the natural aging process has been reported by some researchers [1, 2, 19, 20]. Matsuo et al. [13, 21–23] used wood that was heat treated at 90–180 °C under dry conditions accompanied by thermal oxidation to simulate archaeological wood. They suggested that wood aging is a mild thermal oxidation and concluded that kinetic analysis using the TTSP method can be applied to wood color characteristics that result from heat treatment. Thus, we expect that kinetic analysis with PCA analysis for NIR spectra can be also used for the simulation of wood aging. To this end, further inspection is required that considers the change in the NIR spectra of wood subjected to thermal treatment under wet conditions, UV irradiation (light degradation) and fungus treatment.

This study showed that kinetic analysis can be applied to NIR second-derivative bands or PCA score calculated from spectra and prediction of these changes with thermal treatment time at least up to 180 °C. As degradation process of wood involves multiple reactions, PCA score which reflects such a complex reaction was a good indicator for the prediction of thermal treatment by TTSP method.

4 Conclusion

Kinetic analysis successfully explains the change in the second-derivative spectral bands and PCA score calculated from the second-derivative NIR spectra of thermally treated Sugi at temperatures of 90, 120, 150 and 180 °C. The PC1 and PC2 scores were well fitted by logistic function, although the PC3 and PC4 scores were fitted by cubic function. The determination coefficient between the

measured PC2 score and that estimated from the master curve and a shift factor was 0.99. The apparent activation energy calculated from the PC2 score was 116 kJ mol^{-1}. The apparent activation energy for second-derivative bands was between 99 and 140 kJ mol^{-1}. This study showed that kinetic analysis can be applied to NIR second-derivative band or PCA score calculated from spectra and prediction of these changes with thermal treatment time at least up to 180 °C.

References

1. B. Esteves, H.M. Pereira, BioResources **4**, 370 (2009)
2. B. Esteves, H. Pereira, Holz. Rod. Werkst. **66**, 323 (2008)
3. R. Mehrotra, P. Singh, H. Kandpal, Thermochim. Acta **60**, 507 (2010)
4. H. Bächle, B. Zimmer, E. Windeisen, G. Wegener, Wood Sci. Technol. **44**, 421 (2010)
5. H. Bächle, B. Zimmer, G. Wegener, Wood Sci. Technol. **46**, 1181 (2012)
6. E. Windeisen, H. Bächle, B. Zimmer, G. Wegener, Holzforschung **63**, 773 (2009)
7. F. Thurner, U. Mann, Ind. Eng. Chem. Process Des. Dev. **20**, 482 (1981)
8. T. Cordero, J.M. Rodrǐguez-Maroto, F. Garcǐa, J.J. Rodrǐguez, Thermochim. Acta **191**, 161 (1991)
9. J.J.M. Órfão, F.J.A. Antunes, J.L. Figueiredo, Fuel **78**, 349 (1999)
10. D.K. Shen, S. Gu, K.H. Luo, A.V. Bridgwater, M.X. Fang, Fuel **88**, 1024 (2009)
11. G. Goli, B. Marcon, M. Fioravanti, Wood Sci. Technol. **48**, 1303 (2014)
12. H.Z. Ding, Z.D. Wang, Cellulose **14**, 171 (2007)
13. M. Matsuo, K. Umemura, S. Kawai, J. Wood. Sci. **60**, 12 (2014)
14. M. Schwanninger, J.C. Rodrigues, K. Fackler, J. Near Inf. Spec. **19**, 287 (2011)
15. N. Todorovic, Z. Popovic, G. Milic, Wood Sci. Technol. **49**, 527 (2015)
16. T. Inagaki, K. Mitsui, S. Tsuchikawa, Appl. Spectrosc. **62**, 1209 (2008)
17. K. Mitsui, T. Inagaki, S. Tsuchikawa, Biomacromolecules **9**, 268 (2008)
18. T. Inagaki, H. Yonenobu, S. Tsuchikawa, Appl. Spectrosc. **62**, 860 (2008)
19. X. Zou, T. Uesaka, N. Gurnagul, Cellulose **3**, 243 (1996)
20. X. Zou, T. Uesaka, N. Gurnagul, Cellulose **3**, 269 (1996)
21. M. Matsuo, M. Yokoyama, K. Umemura, J. Gril, K. Yano, S. Kawai, Appl. Phys. A **99**, 47 (2010)
22. M. Matsuo, M. Yokoyama, K. Umemura, J. Sugiyama, S. Kawai, J. Gril, S. Kubodera, T. Mitsutani, H. Ozaki, M. Sakamoto, M. Imamura, Holzforschung **65**, 361 (2011)
23. M. Matsuo, K. Umemura, S. Kawai, J. Wood. Sci. **58**, 113 (2012)